Supplement of Earth Syst. Sci. Data, 18, 5583–5599, 2026
https://doi.org/10.5194/essd-18-5583-2026-supplement

Open Access Earth System Science Data

Supplement of

Mapping paddy rice distribution and cropping intensity in South and Southeast Asia (1995–2024) at 30 m resolution

Zizhang Zhao et al.

Correspondence to: Geli Zhang (geli.zhang@cau.edu.cn)

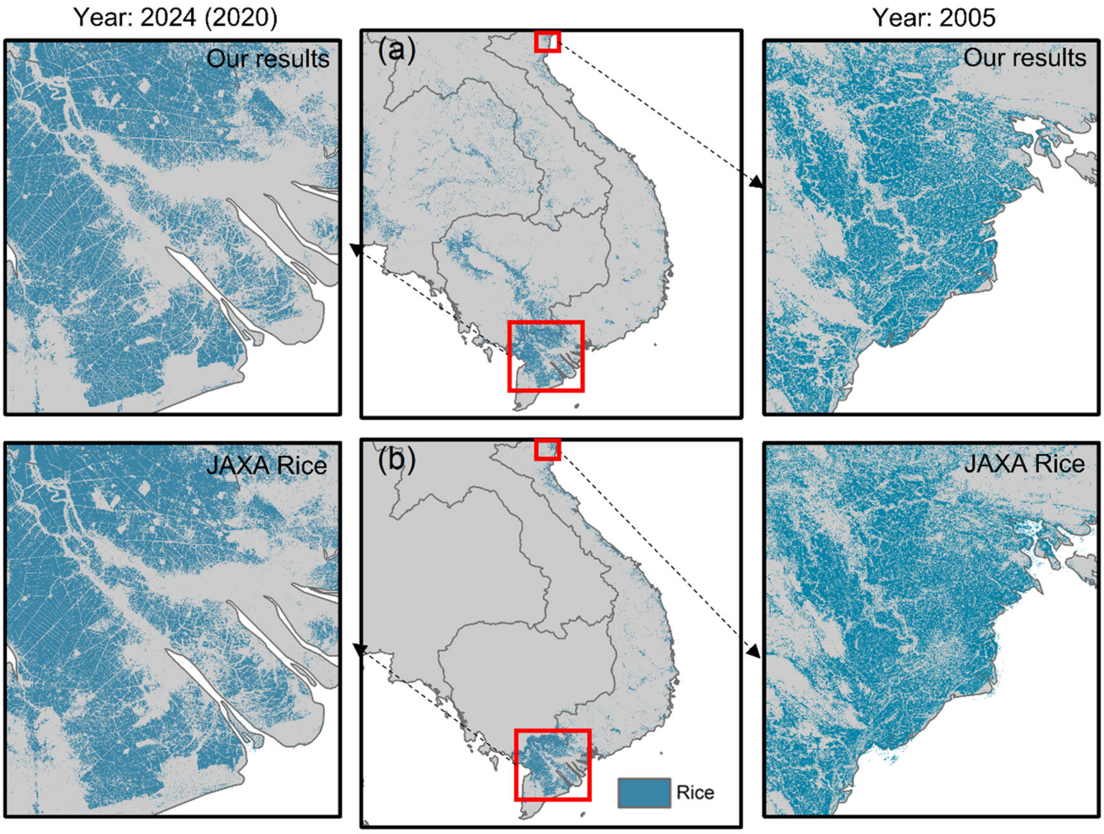

Fig. S1. Comparison of rice mapping results between our method and JAXA Rice product in Vietnam for the years 2024 (2020) and 2005, with zoomed-in views of selected regions.

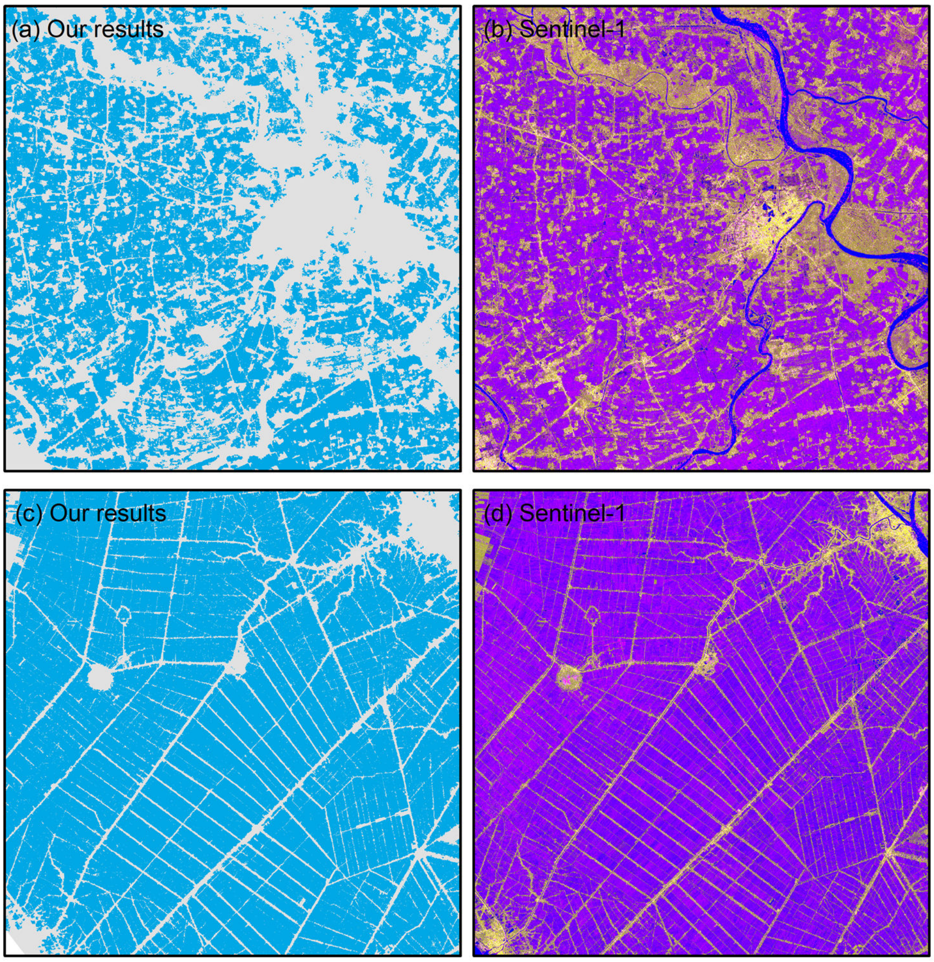

Fig. S2. Spatial comparison of rice distribution maps and reference imagery over selected regions in Vietnam, highlighting consistency between optical- and SAR-based rice detection.

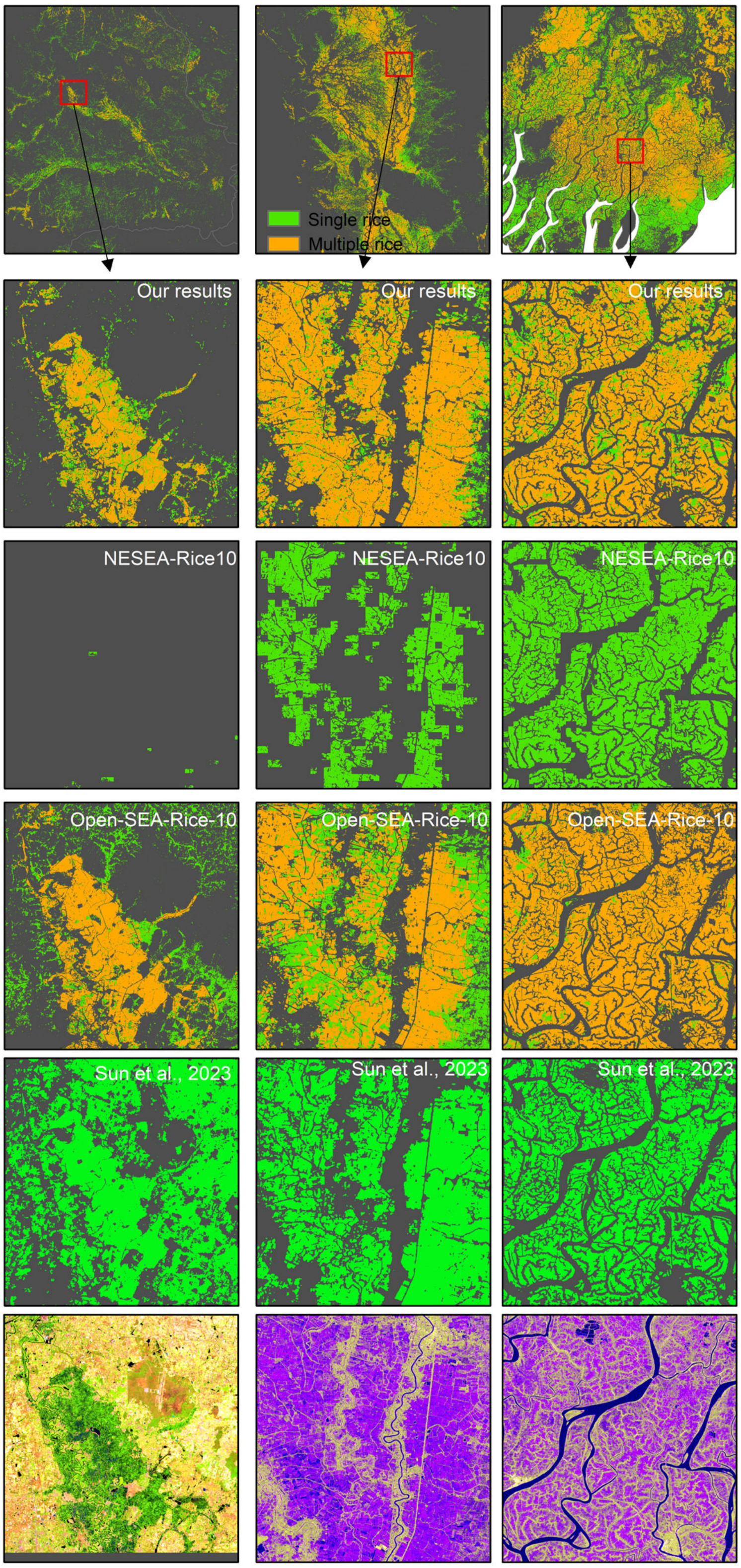

Fig. S3. Field-scale comparison of rice distribution and cropping-intensity products with corresponding reference imagery. The top row shows regional overview maps from this study, with red boxes indicating the selected zoom-in regions. The following rows provide field-scale comparisons among our results, NESEA-Rice10, Open-SEA-

Rice-10, and Sun et al. (2023). Green indicates single-season rice or rice extent, and orange indicates multiple-season rice where available. The bottom row shows corresponding reference imagery used for qualitative evaluation: the first column uses a Sentinel-2 false-color composite, while the second and third columns use Sentinel-1 SAR pseudo-color composites. These reference images help assess the spatial consistency of rice-field boundaries and multiple-season rice patterns across different products.

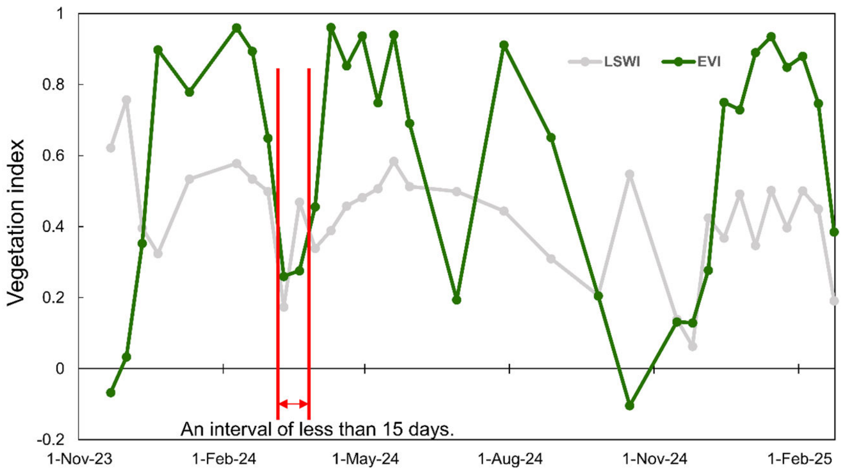

Fig. S4. Time series of Land Surface Water Index (LSWI) and Normalized Difference Vegetation Index (NDVI) for a representative rice pixel in the Mekong Delta, Vietnam, from November 2023 to February 2025 with a red vertical line indicating an interval of less than 15 days

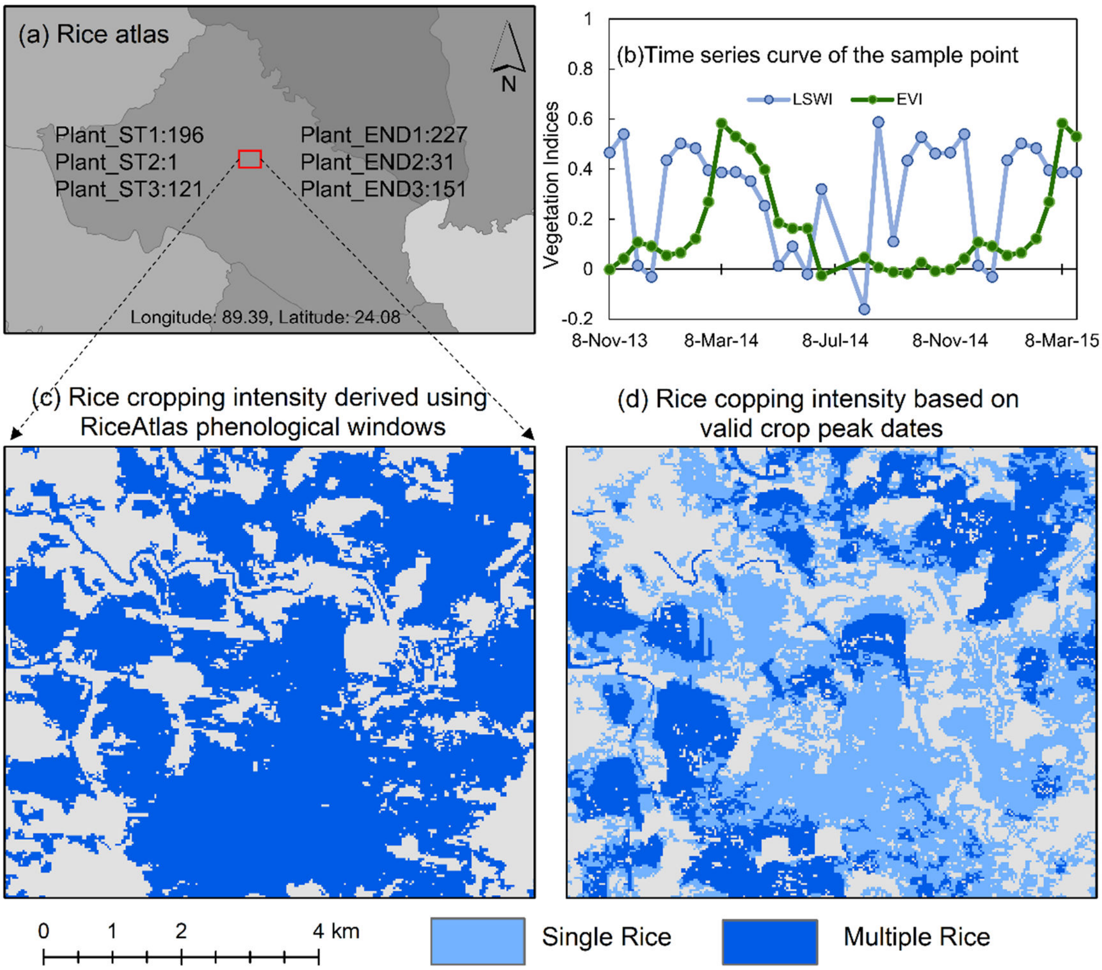

Fig. S5. Time-series comparison between the RiceAtlas-based approach and the proposed peak-detection framework at an example location affected by seasonal flooding.

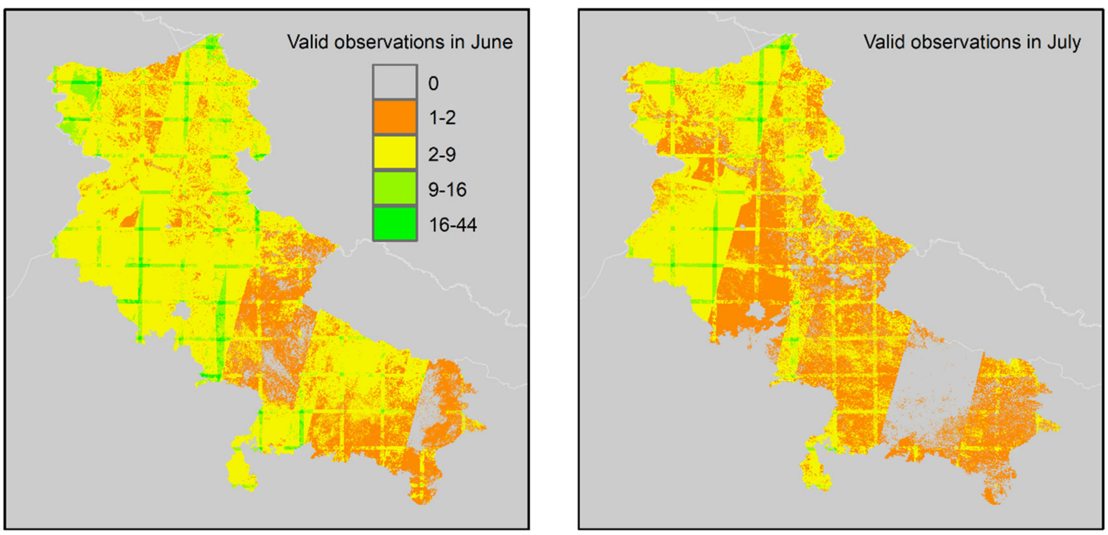

Fig. S6. Spatial distribution of valid satellite observations in the Mekong Delta, Vietnam, for June (left) and July (right).

Table S1. Confusion matrices for the independent validation of rice mapping results in 1995, 2005, and 2015.

Year	Overall Accuracy	User Accuracy	Producer Accuracy	F1 Score
2015	0.8018	0.8785	0.7774	0.8249
2005	0.8748	0.8966	0.8000	0.8456
1995	0.7890	0.9675	0.6980	0.8109

Whittaker Smoothing Sensitivity Analysis

To evaluate the sensitivity of the Whittaker smoothing algorithm to the smoothing parameter λ, a comparative analysis was conducted using λ values of 100, 300, 500, 1000, and 2000. As shown in the figure, although the degree of smoothness varies noticeably with λ, the detected peak date remains consistently stable at 26 February across all tested values.

Differences in λ are more likely to affect the identification of certain phenological metrics, such as the start of season (SOS) and the end of season (EOS). However, this study does not rely on extracting precise phenological transition dates. Instead, we only identify the relative peak date within each rice growth cycle and then construct a fixed temporal window around this peak for subsequent classification.

Because the timing of the maximum NDVI value (the key feature we use) shows no meaningful shift within the tested range, minor changes in curve shape caused by different λ values do not alter the position of the peak or the resulting temporal window. Therefore, as long as λ falls within a reasonable range (e.g., 300–500), the smoothing process does not substantially influence the final accuracy of the rice mapping results. The value λ = 300 was ultimately adopted in this study.

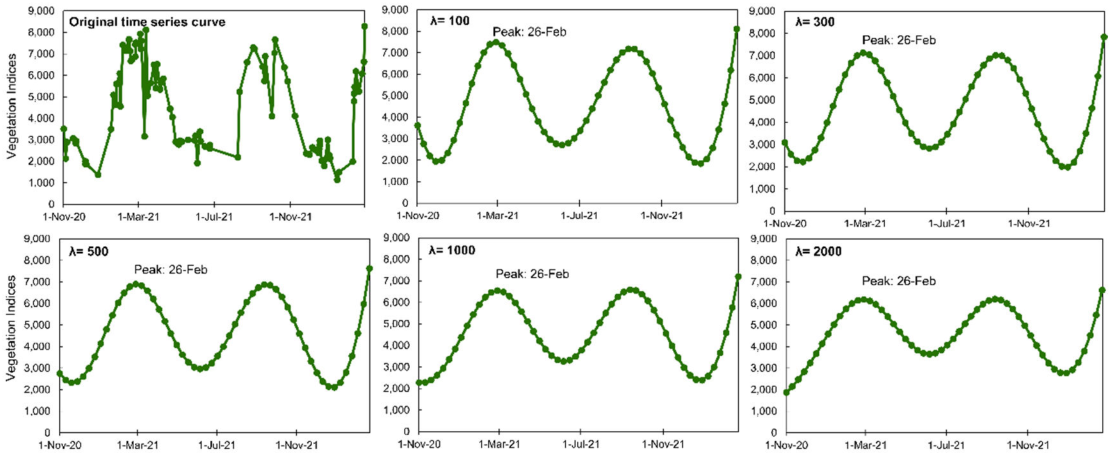

Fig. S7. Whittaker smoothing sensitivity analysis on NDVI time series curve (λ = 100, 300, 500, 1000, 2000). Note: In the intermediate processing step, the original NDVI values were multiplied by 1000 (i.e., the plotted vegetation indices represent NDVI × 1000).

Supplementary Note. Annual-versus-composite assessment of rice cropping intensity

Rationale and experimental design.

The use of multi-year image compositing is necessary for long-term optical-based rice mapping in South and mainland Southeast Asia, where persistent cloud cover, monsoon rainfall, and sparse historical Landsat observations often limit the availability of valid images during key rice phenological stages. However, multi-year compositing may also smooth interannual variability or obscure year-to-year changes in rice distribution and cropping intensity. To quantify this potential effect, we conducted an annual-versus-composite experiment for the recent data-rich period of 2021–2025, during which both Landsat and Sentinel-2 observations were available.

In this experiment, the same phenology-based workflow used for the main product was applied on a strictly single-year basis. For each year from 2021 to 2025, only Landsat and Sentinel-2 observations acquired within that calendar year were used to generate annual rice-intensity maps. These annual products were then compared with the corresponding five-year composite product to evaluate the influence of compositing on rice extent, cropping-intensity classes, and map stability. The analysis was designed as a quantitative uncertainty assessment rather than an independent ground-truth validation, because both annual and composite products were generated using the same mapping framework.

To better interpret the results, we considered two broad agricultural zones with distinct rice production systems. The first zone includes mainland Southeast Asia and Bangladesh, where rice is the dominant staple crop and multi-season rice systems are widespread, particularly in deltaic and irrigated lowland regions. The second zone includes India and Pakistan, where rice–wheat rotation, complex mixed-cropping systems, and a larger proportion of non-rice croplands make annual optical-based mapping more sensitive to observation availability and phenological timing.

Annual variability in rice extent and cropping intensity.

The annual mapping results from 2021 to 2025 showed that the broad spatial extent of rice cultivation was comparatively stable at the regional scale. Across the study area, the mean total rice extent was 50.67 Mha, with an annual range of 47.11–54.75 Mha and a coefficient of variation of 6.7% (Table S2). By contrast, cropping-intensity classes showed larger interannual variability. The coefficient of variation was 5.8% for single-season rice, 15.4% for double-season rice, and 31.9% for triple-season rice. This contrast indicates that single-year optical mapping is more sensitive to missing observations when retrieving rice cropping intensity than when delineating the broad rice-growing extent.

The five-year composite product had a total rice extent of 56.74 Mha, compared with 50.67 Mha for the annual mean. However, the difference in intensity-weighted rice area was more moderate, increasing from 69.75 Mha in the annual mean to 73.44 Mha in the composite product, corresponding to a relative difference of +5.3% (Table S3). These results suggest that the main uncertainty introduced by multi-year compositing lies in the allocation and detectability of single-, double-, and triple-season rice classes, rather than in a simple expansion or contraction of the overall harvested-area proxy.

Mainland Southeast Asia and Bangladesh.

For mainland Southeast Asia and Bangladesh, the annual maps from 2021 to 2025 showed relatively stable core rice-growing boundaries (Fig. S8). Interannual differences were mainly concentrated in cropping intensity rather than in the spatial boundary of rice cultivation. Local fluctuations were visible in some rainfed and transitional zones, such as parts of eastern Thailand, but these differences did not substantially alter the dominant regional distribution of rice. Compared with the single-year annual maps, the five-year composite product did not introduce obvious large-scale spatial artifacts and generally preserved the main rice-growing patterns while reducing the influence of single-year observation gaps.

Detailed local examples from the Ayeyarwady Delta and Mekong Delta further illustrate why the five-year composite product may identify more multiple-season rice in intensive rice-producing regions (Fig. S9). These areas are characterized by high cropping intensity and short intervals between consecutive rice seasons. In some triple-season systems, one cropping cycle may begin in October or November of the preceding calendar year and end in the following year. When annual mapping is restricted to a single calendar year, valid observations may be insufficient during these transitional periods, causing one rice season to be missed or downgraded. The five-year composite increases the probability of capturing the complete sequence of flooding, transplanting, and peak-growth signals, thereby improving the detectability of multiple-season rice. Therefore, the larger multiple-season rice area in the composite product should be interpreted as improved detection of multi-season phenological signals within the composite period, rather than as direct evidence of annual expansion of rice fields.

India and Pakistan.

In India and Pakistan, interannual discrepancies among annual maps were more pronounced than in mainland Southeast Asia and Bangladesh (Fig. S10). This difference is expected because the region includes complex rice–wheat rotation systems, mixed agricultural landscapes, and large areas of non-rice croplands. In northern India, the rice transplanting period typically coincides with the monsoon season, during which heavy cloud cover and atmospheric haze substantially reduce the availability of valid optical observations. As a result, single-year optical mapping can produce unstable results when key flooding or early-growth signals are missed.

Local examples from eastern and southern India show that several annual maps were affected by observation gaps, cloud-masking artifacts, or incomplete seasonal coverage (Figs. S11–S13). In eastern India, some annual products exhibited striping or omission patterns associated with limited valid observations. In southern India, annual maps generally captured the main double-season rice patterns, but localized discrepancies still occurred when valid optical observations were missing during key phenological windows. These examples indicate that the apparent interannual differences in single-year maps are not solely attributable to actual changes in farmer behavior or crop rotation; they also reflect the instability of optical-based rice detection under data-scarce conditions.

We further evaluated annual and composite mapping results over northern India using visually interpreted validation samples. The composite product achieved an overall accuracy of 0.855 and an F1-score of 0.861 (Table S4). Although some annual products achieved comparable or slightly higher accuracy in individual years, other annual maps showed clear degradation under limited observation conditions. For example, the 2022 annual product had an overall accuracy of 0.788, and the 2025 product had a producer accuracy of 0.610. These results highlight the trade-off between temporal specificity and mapping stability: single-year products may better represent true annual conditions when observations are sufficient, but they can suffer from severe omission errors when key phenological phases are not observed.

Implications for interpreting the five-year composite products.

The annual-versus-composite experiment demonstrates that the five-year compositing strategy provides a practical compromise for long-term rice mapping in cloud-prone monsoon regions. The broad rice-growing extent is relatively stable across annual products, whereas the classification of cropping intensity is more sensitive to annual observation availability. Multi-year compositing increases the probability of capturing diagnostic rice phenological and flooding signals, especially for double- and triple-season rice systems with short or cross-year crop cycles. At the same time, compositing may smooth localized interannual changes in crop rotation, management practices, or temporary land-use shifts.

Therefore, the rice products generated in this study should be interpreted as multi-year composite-period rice maps rather than strict annual maps. This distinction is particularly important for cropping intensity. The rice extent layer represents rice occurrence detected within the corresponding composite period, whereas the cropping-intensity layer represents the dominant or detectable rice intensity captured from the multi-year time series. For applications requiring exact year-specific crop management information, such as annual food-security assessment or year-specific crop rotation analysis, users should interpret the cropping-intensity classes with caution. For long-term regional assessments of rice distribution, cropping-intensity patterns, methane emissions, and water-resource demand, the five-year composite products provide a more spatially stable and observation-supported representation than single-year optical maps, especially for historical periods when valid Landsat observations were scarce.

Table S2. Annual variability of rice extent and cropping intensity during 2021–2025.

This table summarizes the annual rice-intensity maps generated using only observations from each individual calendar year. Areas are reported in million hectares (Mha). The coefficient of variation (CV) was calculated across the five annual maps.

Year	Single-season rice	Double-season rice	Triple-season rice	Total rice extent	Intensity-weighted rice area
2021	32.42	14.46	0.56	47.44	63.02
2022	35.05	18.74	0.96	54.75	75.40
2023	30.81	21.18	1.08	53.07	76.41
2024	33.46	16.99	0.56	51.01	69.12

Year	Single-season rice	Double-season rice	Triple-season rice	Total rice extent	Intensity-weighted rice area
2025	30.52	15.49	1.11	47.11	64.81
Mean	32.45	17.37	0.85	50.67	69.75
Range	30.52–35.05	14.46–21.18	0.56–1.11	47.11–54.75	63.02–76.41
CV (%)	5.8	15.4	31.9	6.7	8.7

Table S3. Differences between the 2021–2025 annual mean and the five-year composite product.

Areas are reported in million hectares (Mha). The intensity-weighted rice area was calculated as single-season rice area + 2 × double-season rice area + 3 × triple-season rice area.

Metric	Annual mean 2021–2025	Annual range	Five-year composite product	Difference	Relative difference (%)
Single-season rice	32.45	30.52–35.05	41.80	+9.35	+28.8
Double-season rice	17.37	14.46–21.18	13.17	−4.20	−24.2
Triple-season rice	0.85	0.56–1.11	1.77	+0.91	+106.6
Total rice extent	50.67	47.11–54.75	56.74	+6.07	+12.0
Intensity-weighted rice area	69.75	63.02–76.41	73.44	+3.69	+5.3

Table S4. Accuracy assessment of annual and five-year composite mapping results in northern India.

The validation samples were visually interpreted using available reference imagery. This table is used to illustrate the trade-off between single-year temporal specificity and multi-year mapping stability under observation-limited conditions.

Product	OA	UA	PA	F1-score
Five-year composite product	0.855	0.942	0.792	0.861
2021 annual product	0.830	0.914	0.729	0.811
2022 annual product	0.788	0.783	0.797	0.789
2023 annual product	0.871	0.877	0.876	0.877
2024 annual product	0.879	0.903	0.861	0.882

Product	OA	UA	PA	F1-score
2025 annual product	0.822	0.975	0.610	0.750

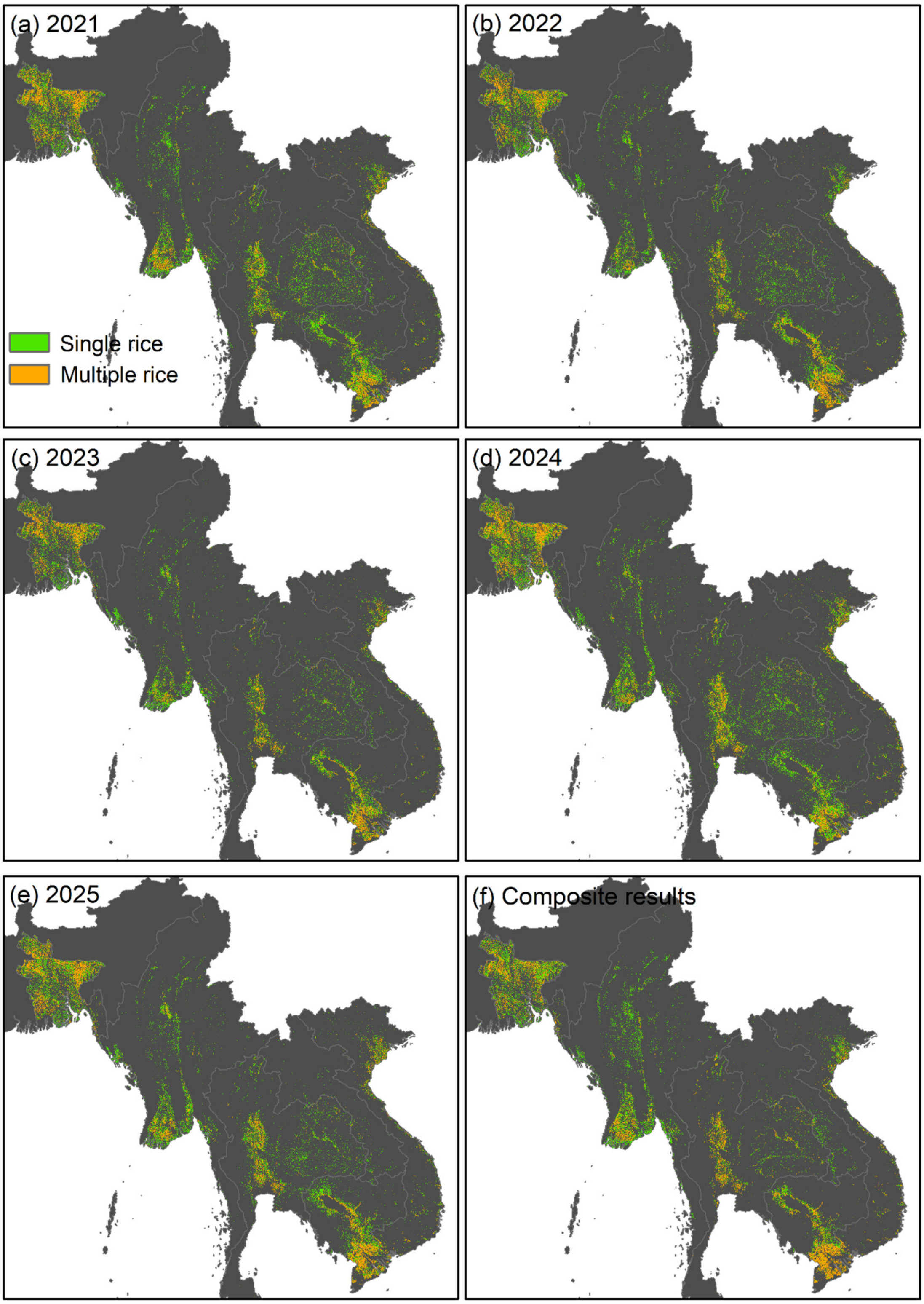

Figure S8. Annual and five-year composite rice cropping-intensity maps for mainland Southeast Asia and Bangladesh during 2021–2025. Panels (a)-(e) display the annual distribution of single- and multiple-season rice derived from single-year observations, while panel (f) presents the five-year composite result using the same algorithm.

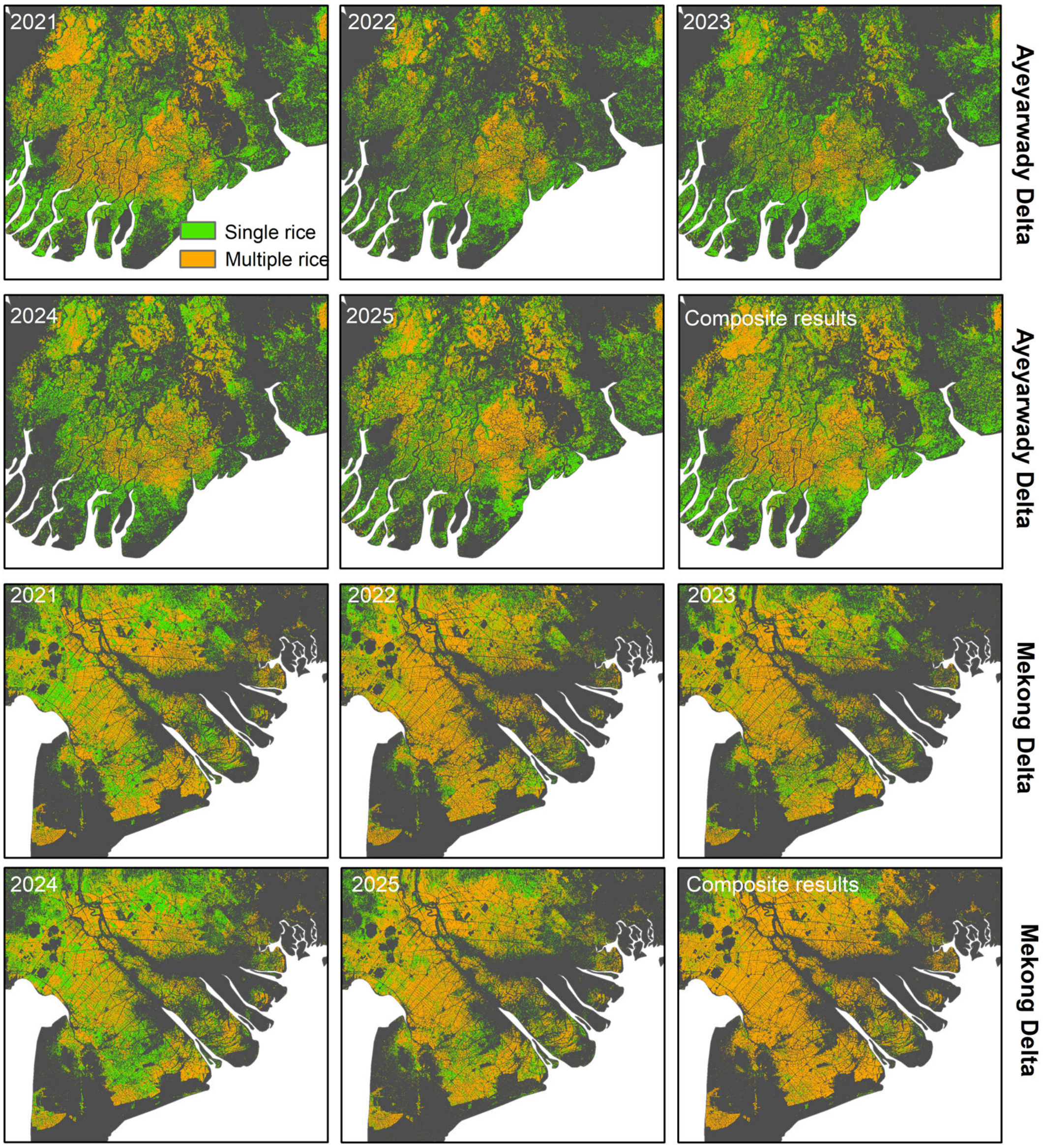

Figure S9. Detailed local views of annual (2021 – 2025) and five-year composite rice cropping intensity maps in typical high-intensity, multi-season rice producing areas of Ayeyarwady Delta (top two rows) and Mekong Delta (bottom two rows).

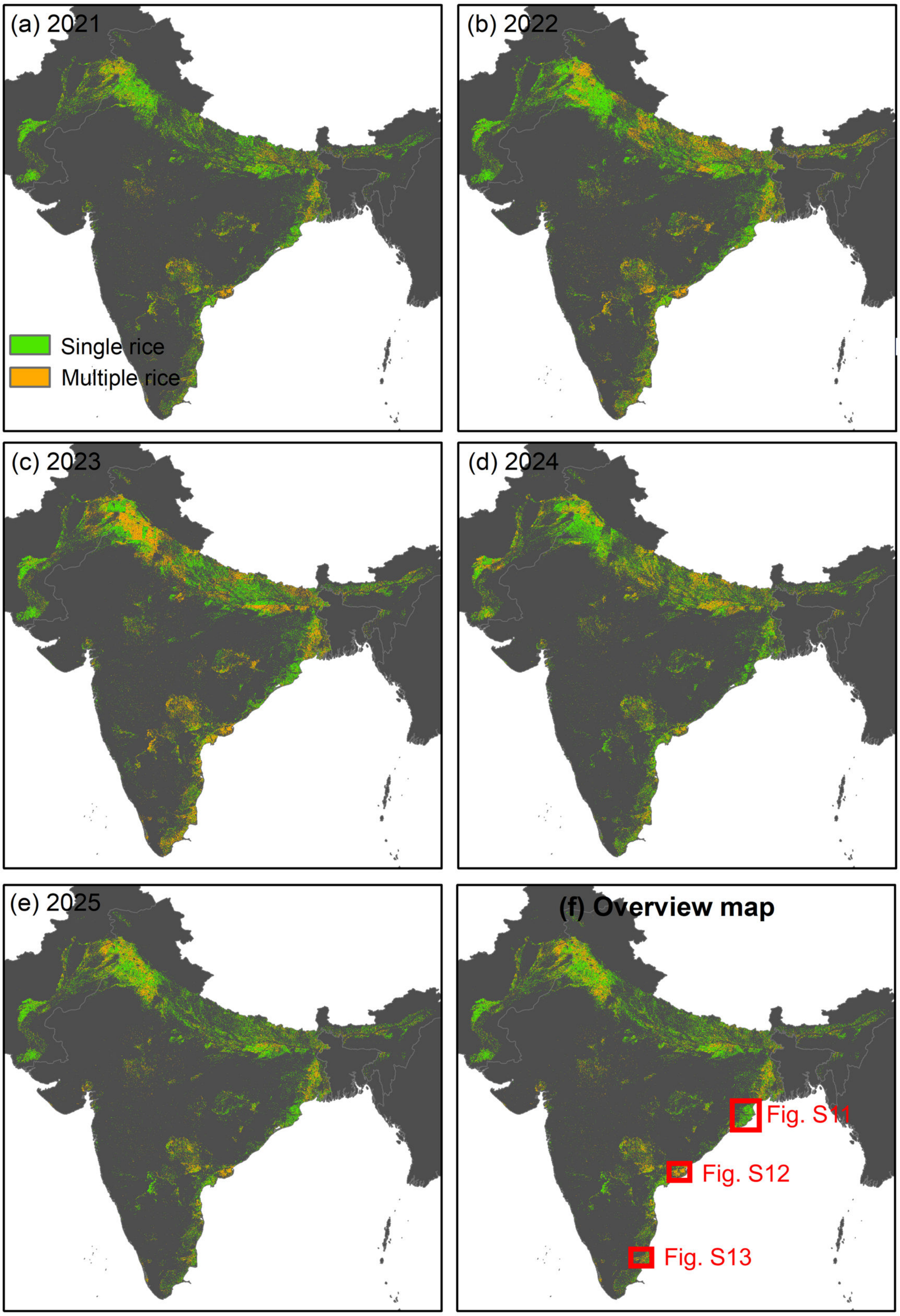

Figure S10. Annual rice cropping-intensity maps for India during 2021–2025. The maps illustrate interannual variations across the subcontinent. An overview locator map is included to indicate the specific spatial extents (red bounding boxes) of the local regions detailed in subsequent figures (e.g., Fig. S11, Fig. S12, Fig. S13).

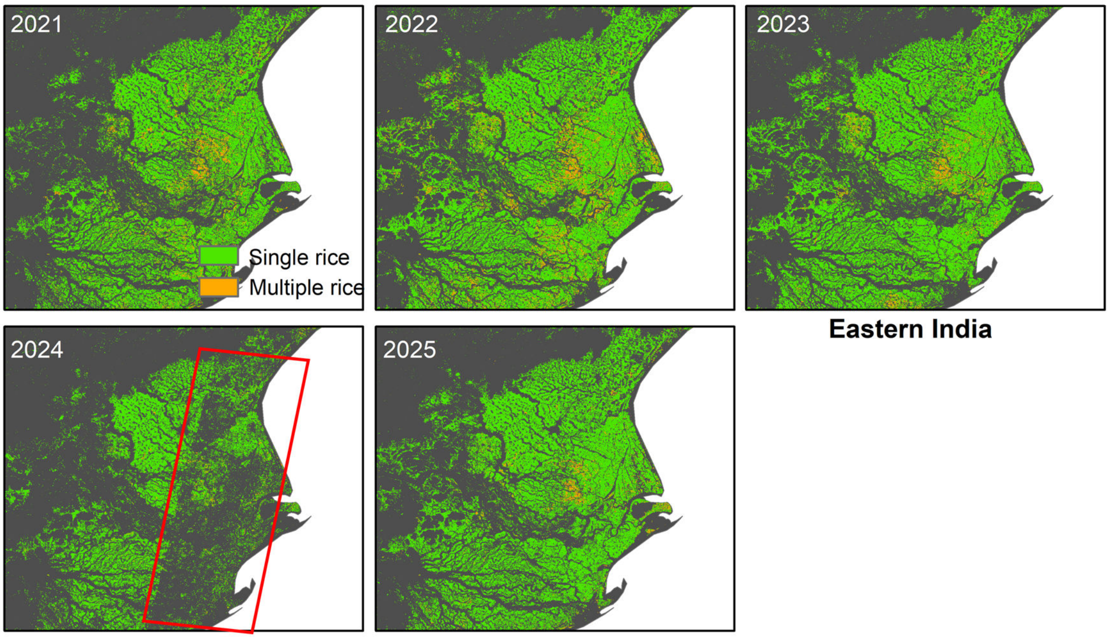

Figure S11. Detailed annual rice cropping intensity maps (2021-2025) for the major rice-producing regions in eastern India. The exact geographical location of this region is indicated by the red bounding box labeled Fig. S10 in the overview map. While the spatial distribution is generally consistent across most years, distinct satellite orbit observation gaps are clearly visible in the 2024 mapping result, highlighting how missing optical data can severely degrade single-year mapping accuracy.

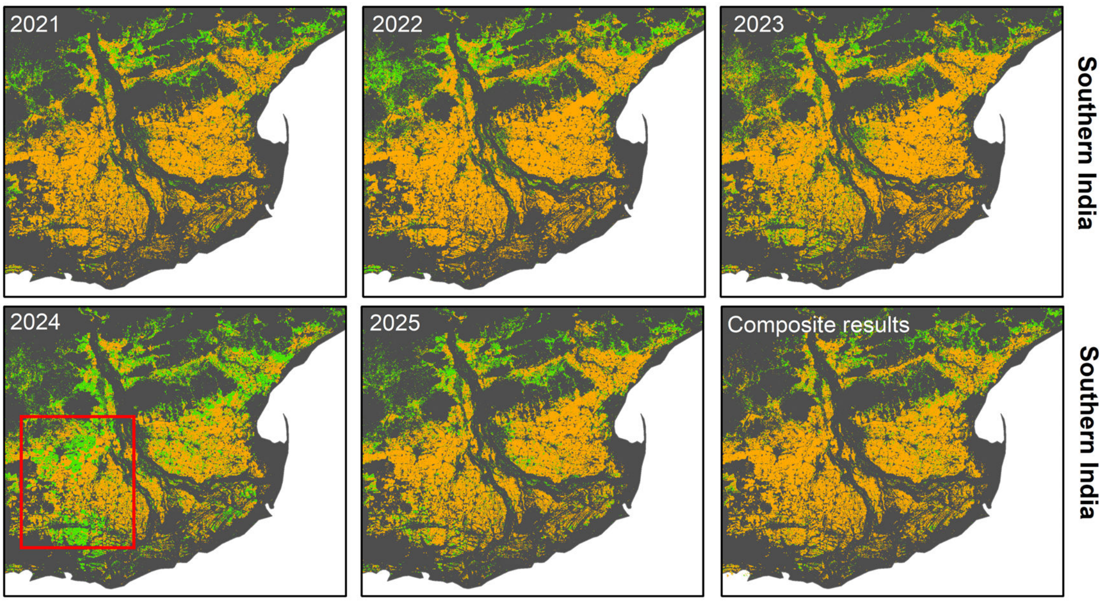

Figure S12. Local annual-versus-composite comparison in a double-season rice region of southern India. The comparison shows that annual maps generally capture the main double-season rice patterns, but localized discrepancies occur when valid observations are insufficient during one of the rice-growing cycles.

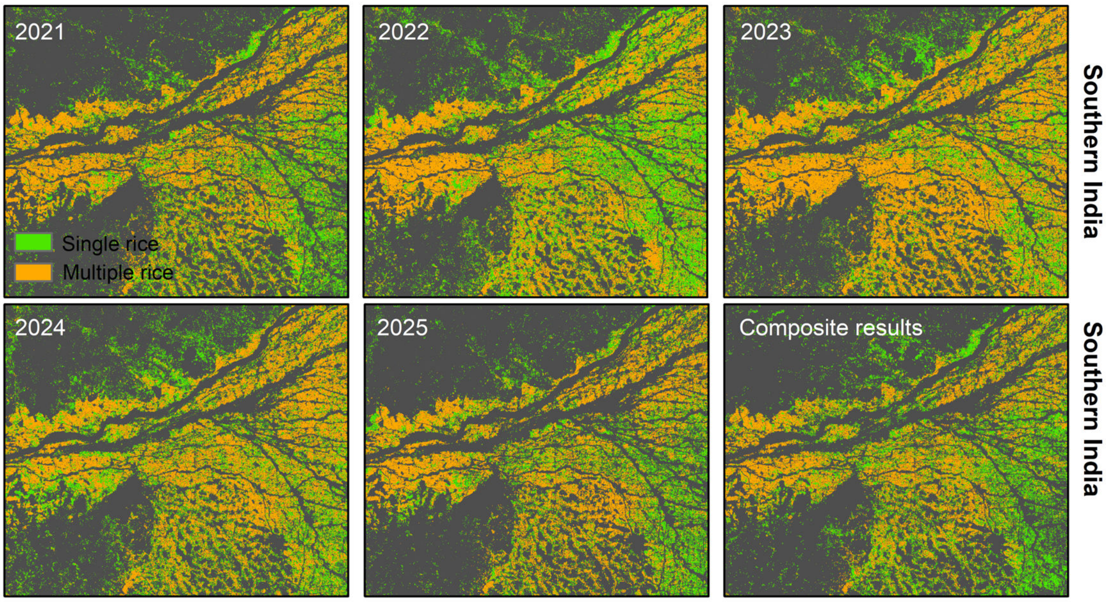

Figure S13. Fine-scale comparison of single- and multiple-season rice from 2021 to 2025 and the five-year composite product in southern India. This example illustrates localized interannual variability in cropping intensity and supports the interpretation that multi-year compositing improves mapping stability while potentially smoothing some year-to-year changes.